CHAOS
Theory and Applications
in Applied Sciences and Engineering

e-ISSN: 2687-4539
RESEARCH ARTICLE
Vol.6 / No.2 / 2024 / pp.131-143
Special Issue (EDIESCA 2023)
https://doi.org/10.51537/chaos.1372066

Opposition to Synchronization of Bistable State in Motif Configuration of Rössler Chaotic Oscillator Systems

J. H. García-López [1,α], **R. Jaimes-Reátegui** [2,α], **G. Huerta-Cuéllar** [3,α] **and D. López-Mancilla** [4,*]

[α]Optics, Complex Systems, and Innovation Laboratory, Centro Universitario de los Lagos, Universidad de Guadalajara, Lagos de Moreno, 47463, Jalisco, Mexico, [*]Control Laboratory, Centro Universitario de los Lagos, Universidad de Guadalajara, Lagos de Moreno, 47463, Jalisco, Mexico.

ABSTRACT This paper presents the study of the opposition to the synchronization of bistable chaotic oscillator systems in basic motif configurations. The following configurations were analyzed: Driver-response oscillator systems coupling, two driver oscillator systems to one response oscillator, and a three-oscillator systems ring unidirectional configuration. The study was conducted using the differential equations representing the piecewise linear Rössler-like electronic circuits; the initial conditions were changed to achieve a bistable characteristic Homoclinic **H**-type or Rössler **R**-type attractor. Analyzing a sweep of the initial conditions, the basin attractor was obtained. It can be observed that each system has a preferred Homoclinic chaotic attractor with any perturbation or change in initial conditions. A similarity analysis based on the coupling factor was also performed and found that the system has a preferentially Homoclinic chaotic attractor.

KEYWORDS
Rössler oscillator
Opposition to synchronization
Complex network
Coupled oscillators

INTRODUCTION

According to the Britain English dictionary, the meaning of the term synchronization is to occur at the same time. This phenomenon is now known as synchronization and represents the adjustment of the rhythm of the oscillations of two or more systems due to the weak interaction between them. Synchronization is commonly understood as a collective state of a coupled system. In general, it indicates the existence of some relation between functions of the different processes due to interaction (Boccaletti *et al.* 2001). Synchronization is also a process during which coupled system adjust their individual frequency in an organized fashion. Synchronization is a process where, due to their interaction or an external driving force, a dynamic system adjusts some properties of their trajectories so that they eventually operate macroscopically coherently.

The first studies on synchronization are historically attributed to the Dutch scientist Christian Huygens who invented two pendulum clocks attached to the same beam supported by two chairs in 1657. Studying synchronization in dynamic systems is extremely important in science and engineering and has numerous applications in many fields, from mechanics and electronics to physics, chemistry, biology, and even economics. Synchronization is ubiquitous in a natural and man-made system (Rosenblum and Kurths 2003; Boccaletti 2008). As examples of synchronization motion that are observed in a real-world system, we can mention a symphony orchestra is synchronized by the conductor, a school of fish changing its shape when attacked by sharks, the unison song of crickets, the synchronous rhythmic flash of fireflies observed in Borneo forest, the spontaneous synchronizations of clapping in a human platea.

Another manifestation of synchronization is the study conducted by Farkas *et al.* (2002) focusing on "La ola," which serves as an example illustrating how synchronization behaviors emerge within complex dynamical systems. Under specific initial conditions, this system transitions from a dormant state with sporadic fluctuations (where most individuals are seated, occasionally with a few raised hands) to a collective action phase. During this phase, the crowd synchronizes coherently by standing up with raised arms and sitting down, creating a phenomenon resembling a traveling wave – commonly known as "La ola" – that periodically traverses the stadium.

In man-made systems, physical devices exist where synchronous behavior enhances overall performance. An example is the Van der Pol electrical circuit (1889-1959), which employed vacuum tubes and discovered that they exhibit stable oscillations. When these circuits were driven by a periodic signal near the limit

Manuscript received: 6 October 2023,
Revised: 15 November 2023,
Accepted: 4 December 2023.

[1]jhugo.garcia@academicos.udg.mx
[2]rider.jaimes@academicos.udg.mx (**Corresponding author**)
[3]guillermo.huerta@academicos.udg.mx
[4]didier.lopez@academicos.udg.mx

cycle, their oscillation frequency became entrained by the external driven. This discovery had a great deal of practical importance because the vacuum tube was, at that time, the basic element of the radio communications systems (Pol and Mark 1927).

Furthermore, an arrangement of Josephson junctions exhibits heightened output power when these junctions oscillate in synchrony, as Barbara et al. (1999) demonstrated. Synchronous periodic states have been documented in numerous dynamic processes across diverse scientific and engineering domains. For a comprehensive exploration of this topic, we recommend readers consult the outstanding monograph authored by Pikovsky et al. (2001). Therefore, the examination of synchronization within complex systems holds a dual significance: from a theoretical standpoint, it provides valuable insights into understanding natural phenomena, and from a technological point of view, it proves to be advantageous for the development of high-performance devices and systems. During these years, chaotic synchronization has attracted great interest in applications such as the design of private and secure communication systems from the paper by Sharma and Ott (2000), to Méndez-Ramírez *et al.* (2023).

Currently, various forms of chaos synchronization can be distinguished. These include Complete Synchronization: The most robust form of synchronization where the state variables of two systems perfectly coincide Pikovsky *et al.* (2001); Phase Synchronization: Which involves a phase difference between chaotic oscillations locked within a range of 2π, representing the weakest manifestation of synchronization in chaotic systems Pecora and Carroll (1990); Antiphase Synchronization: Defines a state where the variables of two interacting systems have the same amplitude but differ in sign Rosenblum *et al.* (1996); Lag Synchronization: Characterized by the coincidence of two chaotic trajectories with a constant time lag Liu *et al.* (2006); Anticipating Synchronization: The opposite of lag synchronization, wherein chaotic trajectories coincide with a constant anticipated time Rosenblum *et al.* (1997); Generalized Synchronization: Involves trajectories of coupled systems that exhibit a specific functional dependence on each other, often utilized to describe synchronous behavior in coupled non-identical systems Rulkov *et al.* (1995). Additionally, there are unstable synchronization states like Intermittent Synchronization, which occurs when any form of synchronization is intermittently interrupted by asynchronous oscillations or the system changes synchronization type periodically, such as switching between phase synchronization and lag synchronization reported by Gauthier and Bienfang (1996); Buldú *et al.* (2006); Pisarchik and Jaimes-Reategui (2005).

Most research on synchronization has primarily focused on monostable systems, which are relatively straightforward dynamical systems characterized by a single attractor when they are uncoupled. However, the prediction of synchronization in multistable systems remains a topic of significant debate, even in seemingly uncomplicated systems like iterative maps. Multistability is a phenomenon that arises in dissipative systems when multiple stable attractors coexist for a specific set of system parameters. This phenomenon has been observed across various scientific domains, including electronics Maurer and Libchaber (1980), optics Brun *et al.* (1985), mechanics Stewart *et al.* (1986), and biology Foss *et al.* (1996). The mechanisms underlying multistability can be diverse, encompassing delayed feedback and homoclinic tangencies in weakly dissipative systems Boccaletti *et al.* (2018). Nonetheless, despite potential differences in the origins of multistability, multistable systems share several common traits. They all exhibit an extremely high sensitivity to initial conditions, where even the slightest perturbations can significantly change the final attractor state. Additionally, their qualitative behavior often undergoes dramatic shifts with only minor parameter variations Boccaletti *et al.* (2018).

Recently, Ahmed *et al.* (2016) conducted a study on robust synchronization in multistable systems evolving on manifolds within an Input-to-State Stability framework. Parallelly, Pm and Kapitaniak (2017) explored synchronization in coupled multistable systems featuring hidden attractors. Additionally, Khan *et al.* (2017) achieved the design of multistable systems through partial synchronization. It is noteworthy that highly multistable synchronized systems can be engineered, wherein all states of one system synchronize with their corresponding states in the other system, as demonstrated by Chakraborty and Poria (2019) and Khan *et al.* (2021). Furthermore, Dudkowski *et al.* (2021) illustrated that multistable synchronous states, encompassing in-phase, anti-phase, and phase-locked synchronization, can emerge based on parameters and initial conditions.

Moreover, Moskalenko *et al.* (2021) made a significant contribution by discovering multistability within the intermittent generalized synchronization regime in unidirectionally coupled chaotic systems. Additional noteworthy work on synchronization in multistable systems has been conducted by Ruiz-Silva *et al.* (2021); Vaidyanathan *et al.* (2022). Similarly, the synchronization of chaotic oscillator system with the application to new technologists has become an area of great importance as it allows us to perform information security analysis in various communication schemes, such as information encryption, data hiding, secure wireless communication, machine-to-machine communication, watermarking, synchronization of chaos, image encryption by Rodríguez-Orozco *et al.* (2018); García-Guerrero *et al.* (2020); Sarosh *et al.* (2022) and Trujillo-Toledo *et al.* (2023).

Nevertheless, developing the states within multistable systems when these systems are coupled remains a largely unresolved question, particularly when dealing with complex scenarios like the coupling of three chaotic bistable systems arranged in a motif configuration. One may naturally speculate about the behavior of the motif system as the coupling strength is increased. It might seem intuitive that the motif system would initially adjust its state to that of one of the bistable systems, transforming the problem into a well-understood case involving identical chaotic monostable systems. However, this simplistic view only captures part of the truth. In this context, the synchronization of multistable systems has received relatively little attention. In a preliminary investigation, we explored the synchronization of two identical chaotic bistable systems coupled in a driver-response oscillator configuration, exemplified by Homoclinic **H**-type or the Rössler **R**-type of the attractor Pisarchik *et al.* (2006).

A homoclinic orbit normally changes its period when the number of loops of the orbit increases or decreases by one saddle point by adding or omitting a loop while varying a control parameter by Pisarchik *et al.* (2005). Our findings revealed that the dynamics of coupled multistable systems are remarkably intricate, encompassing various forms of phase synchronization. The main objective of this work is to study of the opposition to synchronization of bistable chaotic oscillator systems. Our focus here is on synchronizing three coupled chaotic bistable systems arranged in a motif configuration. We examine electronic circuits that resemble Rössler-like systems as previously used by Pecora and Carroll (1990); Carroll and Pecora (1995) in their synchronization studies in chaotic systems.

The next sections of this manuscript are outlined as follows. In Section 2, we provide an overview of the mathematical model. Section 3 offers a detailed examination of the dynamics of an isolated Rössler oscillator, encompassing the bifurcation diagram and the system's time series. Section 4 investigates the synchronization stage of two coupled Rössler oscillators. Section 5 extends this analysis to three coupled Rössler oscillators, presenting the outcomes of numerical simulations and a comprehensive description of the synchronization stages observed. Finally, the conclusions derived from this numerical study are resumed in Section 6.

MATHEMATICAL MODEL

Presenting our analysis without generalization, let us consider the following case: **(a) First case** two identical unidirectional coupled chaotic oscillators, where the driver system is represented by Eqs. (1) and the response system by Eqs. (2), see Fig. 1; **(b) Second case** is shown in the Fig. 2: Three identical coupled chaotic oscillators in network motif configuration, two driver oscillators and one response oscillator represented by the systems of Eqs. (3), Eqs. (4) and Eqs. (5); **(c) Third case** in a ring configuration where all oscillators act together as a driver and response system, represented in this case by the systems of Eqs. (6), Eqs. (7) and Eqs. (8) and shown in the Fig. 3. For all cases, piecewise linear Rössler-like oscillators.

Two identical unidirectional driver-response coupled chaotic oscillators

$$\begin{aligned} \dot{x_1} &= -\delta x_1 - \beta y_1 - \lambda z_1, \\ \dot{y_1} &= x_1 + \gamma y_1, \\ \dot{z_1} &= g(x_1) - z_1, \end{aligned} \tag{1}$$

$$\begin{aligned} \dot{x_2} &= -\delta x_2 - \beta[y_2 - \epsilon(y_2 - y_1)] - \lambda z_2, \\ \dot{y_2} &= x_2 + \gamma[y_2 - \epsilon(y_2 - y_1)], \\ \dot{z_2} &= g(x_2) - z_2, \end{aligned} \tag{2}$$

where

$$g(x_{1,2}) = \begin{cases} 0, \text{ if } x_{1,2} \leq 3 \\ \mu(x_{1,2}), \text{ if } x_{1,2} > 3 \end{cases}$$

with $\delta = 0.05$, $\beta = 0.50$, $\lambda = 1.00$, $\gamma = \frac{R}{R_c}$, (in the experimental circuits $R = 10k\Omega$ and $R_c = 32k\Omega$) and $\epsilon \in [0, 1]$ is the coupling strength.

Three identical coupled chaotic oscillators, two drivers and one response

$$\begin{aligned} \dot{x_1} &= -\delta x_1 - \beta y_1 - \lambda z_1, \\ \dot{y_1} &= x_1 + \gamma y_1, \\ \dot{z_1} &= g(x_1) - z_1, \end{aligned} \tag{3}$$

$$\begin{aligned} \dot{x_2} &= -\delta x_2 - \beta y_2 - \lambda z_2, \\ \dot{y_2} &= x_2 + \gamma y_2, \\ \dot{z_2} &= g(x_2) - z_2, \end{aligned} \tag{4}$$

$$\begin{aligned} \dot{x_3} &= -\delta x_3 - \beta[y_3 - \epsilon(y_3 - y_2 - y_1)] - \lambda z_3, \\ \dot{y_3} &= x_3 + \gamma[y_3 - \epsilon(y_3 - y_2 - y_1)], \\ \dot{z_3} &= g(x_3) - z_3, \end{aligned} \tag{5}$$

where $g(x_{1,2,3}) = \begin{cases} 0, \text{ if } x_{1,2,3} \leq 3 \\ \mu(x_{1,2,3}), \text{ if } x_{1,2,3} > 3 \end{cases}$

with the same values for the parameters δ, β, λ, $\gamma = \frac{R}{R_c}$ and $\epsilon \in [0, 1]$ with similar coupling strength for all systems of equations.

Three identical coupled chaotic oscillators in a unidirectional ring configuration (or a motif configuration in which all oscillators act as driver and response form)

$$\begin{aligned} \dot{x_1} &= -\delta x_1 - \beta[y_1 - \epsilon_1(y_1 - y_3))] - \lambda z_1, \\ \dot{y_1} &= x_1 + \gamma[y_1 - \epsilon_1(y_1 - y_3)], \\ \dot{z_1} &= g(x_1) - z_1, \end{aligned} \tag{6}$$

$$\begin{aligned} \dot{x_2} &= -\delta x_2 - \beta[y_2 - \epsilon_2(y_2 - y_1)] - \lambda z_2, \\ \dot{y_2} &= x_2 + \gamma[y_2 - \epsilon_2(y_2 - y_1)], \\ \dot{z_2} &= g(x_2) - z_2, \end{aligned} \tag{7}$$

$$\begin{aligned} \dot{x_3} &= -\delta x_3 - \beta[y_3 - \epsilon_3(y_3 - y_2)] - \lambda z_3, \\ \dot{y_3} &= x_3 + \gamma[y_3 - \epsilon_3(y_3 - y_2)], \\ \dot{z_3} &= g(x_3) - z_3, \end{aligned} \tag{8}$$

where $g(x_{1,2,3}) = \begin{cases} 0, \text{ if } x_{1,2,3} \leq 3 \\ \mu(x_{1,2,3}), \text{ if } x_{1,2,3} > 3 \end{cases}$

in this third case was used same values for the parameters δ, β, λ, $\gamma = \frac{R}{R_c}$ and $\epsilon_{1,2,3} \in [0, 1]$ with similar coupling strength for all systems of equations.

DYNAMIC OF AN ISOLATED OSCILLATOR

When the driver and response chaotic oscillator, systems of Eqs.1 and Eqs.2 are not coupled ($\epsilon = 0$), each of them exhibits a complex dynamical behavior depending on the control parameter Rc and the initial condition. Fig. 4 (a) shows the bifurcation diagram of the local maximum of the variables x_1 of Eqs.1 as a function of the parameter Rc. This bifurcation diagram is computed under different initial conditions and shows different coexisting attractors. For large values of $28k\Omega < Rc < 141k\Omega$, the variable $x_1 < 3$ the dynamics of the system Eqs.1 or Eqs.2 similar to the classical Rössler oscillator. It exhibit route to the Rössler chaos from a limit cycle with one period and a period-doubling when R_c decreases.

An interesting result was found at relatively low values of the control parameter $R_c < 34k\Omega$, once the variable $x_1 > 3$, a second, different chaotic attractor appears, a Homoclinic-type chaotic attractor coexisting with Rössler-type chaotic attractors. The enlarged part of the bifurcation diagram in the region of small values of $Rc < 34k\Omega$ is shown in Fig. 4 (b). The diagram contains two branches, the red and blue dots, which are obtained by taking different initial conditions. The branch with the red dot corresponds to the typical dynamics of the classical Rössler chaotic attractor, while the branch with the blue dot corresponds to the Homoclinic chaotic attractor. The left column in Fig. 5 represents the Rössler chaotic attractor, in which we plot the time series in Fig. 5 (a), the phase space 5 (c), and the power spectra 5 (e). Fig. 5 right column shows the homoclinic chaotic attractor, where the time series Fig. 5 (b), the phase space 5 (d), and the power spectrum 5 (f) are shown.

In Fig. 6 we show the Poincare section for z_1 of the Eqs.1 or Eqs.2 without coupling. The initial condition for the system Eqs.1 or Eqs.2 representing a homoclinic chaotic attractor **H** is reached using I.C.: $x_{10} = 2.38019$, $y_{10} = -5.31956$ and $z_{10} = 2.32858$, see Fig. 6a and showing a Rössler chaotic attractor **R** is reached using I.C.: $x_{20} = 3.034636$, $y_{20} = -4.64063$ and $z_{20} = 0.00920$ see Fig. 6b. In this Poincare section, the basin attraction of the Rössler and Homoclinic chaotics attractors are presented in green and blue colors, respectively. In both plots of the Fig. 6 we can see that the basin attraction of the homoclinic-type chaotic attractor is much

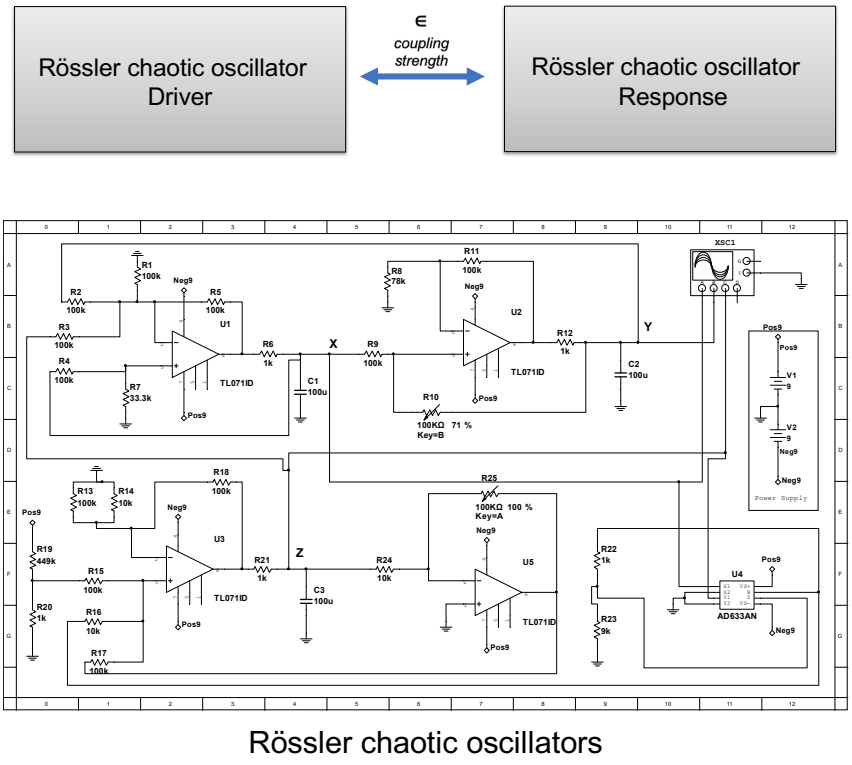

Figure 1 Two identical oscillators, unidirectionally coupled (up) and piecewise linear Rössler-like electronic circuits (down)

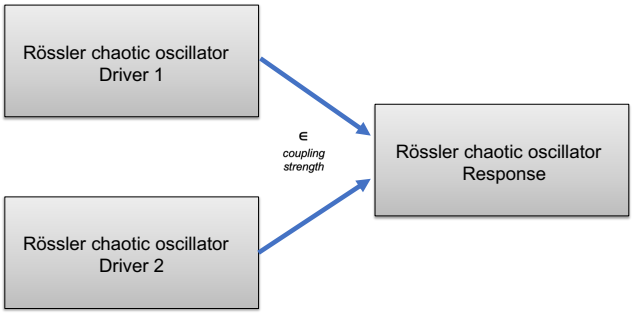

Figure 2 Two drives and one response motif configuration, unidirectionally coupled

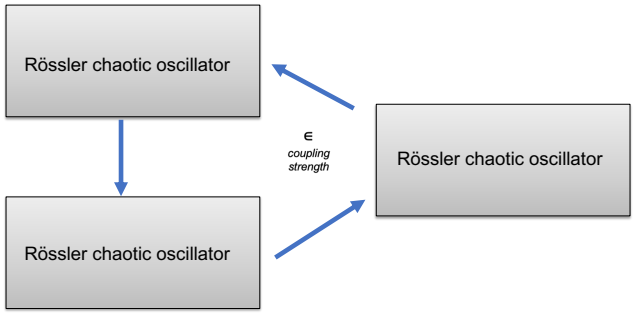

Figure 3 Rössler system unidirectional (A ring of three nodes) motif configuration

larger than the basin attraction of the Rössler-type chaotic attractor and while that the yellow region shows that the system of equation 1 or equation 2 without coupling has no solution.

To study the synchronization of multistable systems, we fixed the control parameter $Rc = 32k\Omega$, where our system exhibits the coexistence of two different chaotic attractors. Then we chose the initial condition for drive system Eqs.1 and response system Eqs.2 so that their chaotics state would be different without coupling $\epsilon_2 = 0$.

Quantitatively, phase synchronization between a pair of oscillators i and j can be characterized by the difference phase between their instantaneous phases Rosenblum and Kurths (2003),

$$\theta_{i,j} = \phi_i - \phi_j \tag{9}$$

$$\phi_{i,j} = arctan(\frac{y_{i,j}}{x_{i,j}}) \tag{10}$$

whereas identical or complete synchronization between a pair of Rössler chaotic oscillators can be determined by the synchronization error Euclidean norma as

$$\left\| e_{ij} \right\| = \sqrt{(x_i - x_j)^2 + (y_i - y_j)^2 + (z_i - z_j)^2} \tag{11}$$

As soon as the oscillator's phases have synchronized, synchronization quality can be characterized by comparing amplitudes

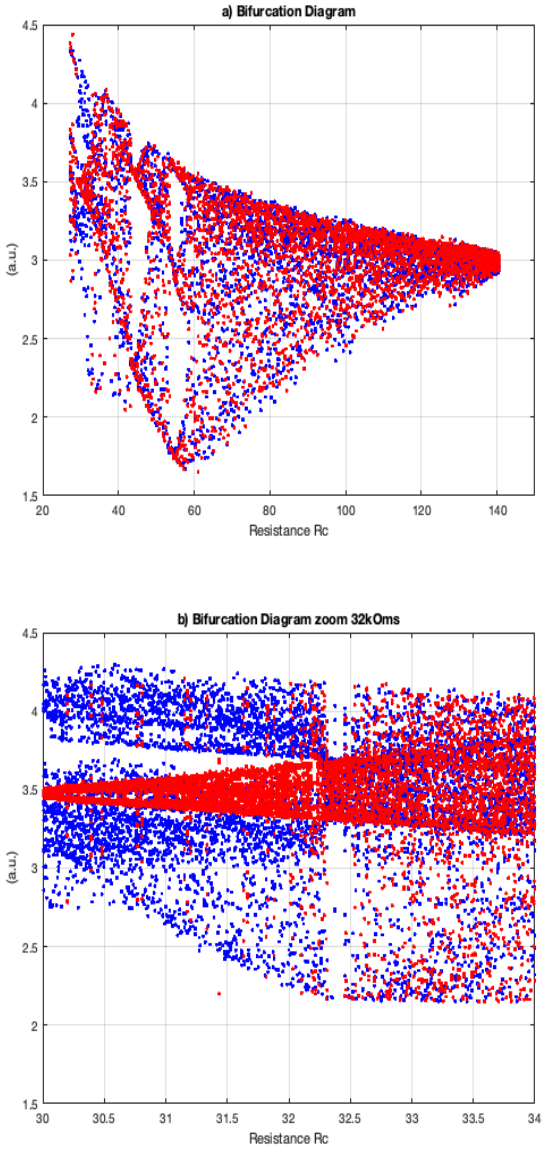

Figure 4 Bifurcation diagram for a Rössler circuit (a) Bifurcation diagram, In blue color from 140 to 0kΩ, and in red from 0 to 140kΩ, (b) A close up of 30 to 34kΩ in the Bifurcation diagram.

of coupled oscillators The commonly used measure for delay synchronization is similarity function S defined as

$$S^2_{i,j}(\tau) = \langle \frac{[x_j(t) - x_i(t+\tau)]^2}{\sqrt{\langle x_j(t)^2 \rangle \langle x_i(t)^2 \rangle}} \rangle \tag{12}$$

where τ is the time shift between two signals. The lower the minimum of similarity function S_{min}, means the better synchronization

SYNCHRONIZATION TWO IDENTICAL RÖSSLER CHAOTIC OSCILLATORS COUPLED

Within this section, phase synchronization in a system of two identical chaotic Rössler oscillators is shown. Specifically, a dynamic system comprising two Rössler chaotic oscillators coupled in a

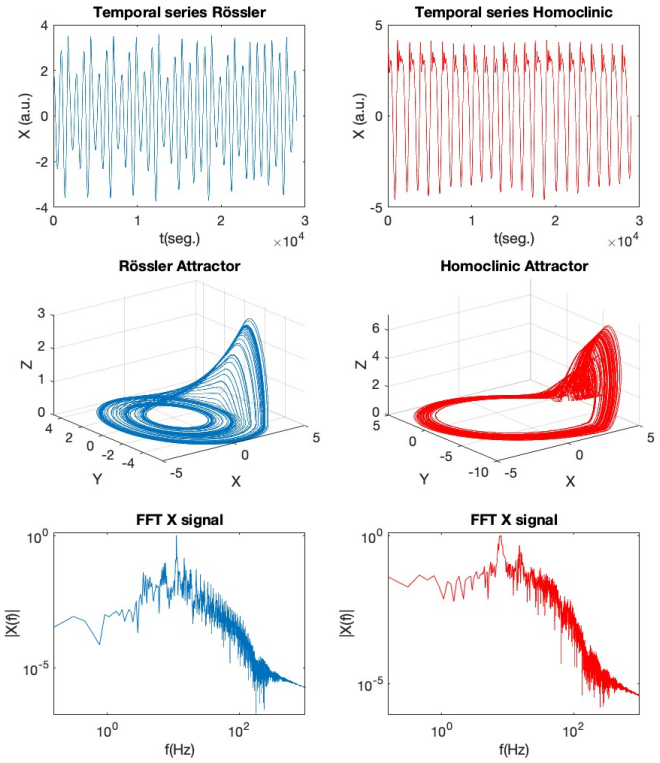

Figure 5 Dinamic of an isolated oscillator (left) Rössler type attractor: Temporal series, space state, and power spectrum, (rigth) Homoclinic type attractor: Temporal series, space state, and power spectrum.

unidirectional manner is examined, as described by Eqs. (1) and Eqs. (2), where $\epsilon \in [0, 1]$. In this setup, the response system, defined by Eqs. (2), is influenced by the variable y_1. It's important to note that the concept of phase lacks a precise definition for complex, chaotic systems, and thus, synchronization stages are interpreted as dimensions. In this context, we delineate three coupling ranges: (i) At very low coupling strength ($\epsilon \ll 1$), the driver signal given by Eqs. (1) is extremely small, resembling noise that doesn't significantly impact the overall structure of the phase space and the attractors in the response system described by Eqs. (2). (ii) the relatively robust chaotic driving from Eqs is at intermediate coupling strength. (1) increases the dimension of the phase space, potentially leading to the emergence of new attractors. And (iii) For very strong coupling ($\epsilon < 1$), the large amplitudes reduce the phase space dimension in the coupled identical multistable system.

To study the synchronization of multistable systems, the parameter R_c is set to $R_c = 32\Omega$, where the system has the coexistence of two different chaotic tractors. Then, we choose the initial condition for the system Eqs.1 representing a homoclinic chaotic or Rössler chaotic attractor. The analysis of synchronization is performed for two different cases: (a) driver system in Homoclinic **H** chaotic attractor and response system in Rössler **R** chaotic attractor, (b) driver system in Rössler **R** chaotic attractor and response system in Homoclinic **H** chaotic attractor.

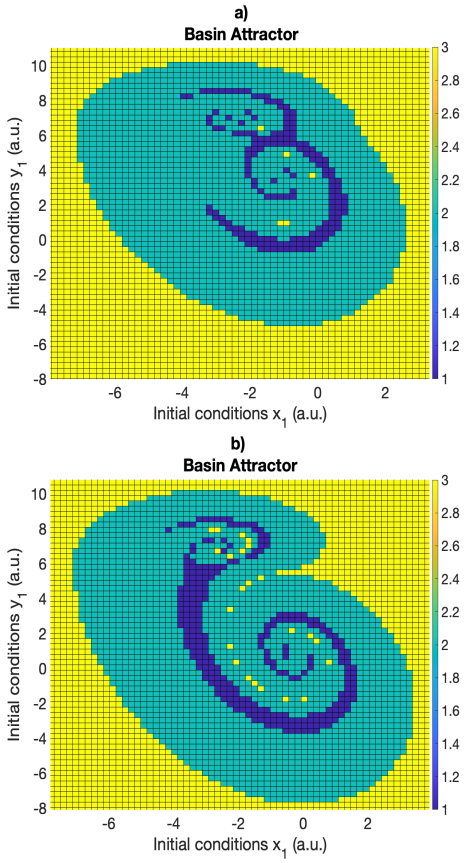

Figure 6 Basin attractor, the area for Homoclinic (green) is bigger than Rössler (blue) behavior. Using initial conditions to a) Homoclinic (**H**) and b) Rössler (**R**) attractor.

Case (a) driver system in Homoclinic chaotic attractor and response system in Rössler chaotic attractor

The time series of the coupled variables x_1 and x_2, the phase difference $\theta_{i,j}$ (see Eq.9) and similarity function $S_{i,j}(\tau)$ (see Eq.12 are shown in Fig. 7 (a)-(c) for a very low coupling strength ($\epsilon = 0.002$). $\theta_{i,j}$ increases linearly with time, indicating no synchronization. At a very low coupling strength ($\epsilon = 0.004$), the driven signal does not affect the response system, and the states are defined by the initial condition. Both oscillators are isolated, and their trajectory occupies a different space phase; see Fig. 5 and fig. 7 (d)-(f). There is a critical value of the coupling strength $\epsilon_c = \epsilon = 0.005$ at which the response oscillator system jumps from the Rössler chaotic attractor **R** to a new Homoclinic chaotic attractor $\mathbf{H}_2$ different from the Homoclinic chaotic attractor $\mathbf{H}_1$ of the driver oscillator system, i.e., the response oscillator system is sensitive to the driver when the response oscillator system switches to the attractors similar to the driver oscillator system, see Fig. 7 (g)-(i). This behavior for parameter $\epsilon_2 = 0.005$ is a precursor of phase synchronization in the multistable system. In Fig. 7 (h) we see how the phase looked $\theta_{i,j}$ approaches $\theta_{i,j} \approx 80$ and while Fig. 7 (i) the minimum S_{min} of the similarity function $S^2_{i,j}(\tau)$ is close to $S \approx 1.1$, which means that the response and the driven system are synchronized in the delayed phase synchronization, see time series 7 (g).

Further increasing the coupling parameter $\epsilon = 0.012$, the phase synchronization is most evident where the response oscillator system remains in the Homoclinic attractor, similar to the driver system's attractor. In the Fig. 7 (j)-(l) we can see that the phase looked $\theta_{i,j}$ decreases to $\theta_{i,j} \approx 20$, see Fig. 7 (k), just as the minimal similarity function S_{min} suffers a decrease Fig. 7 (k) and likewise the response time series is delayed for the driver oscillator time series Fig. 7 (j). While the coupling strength continues to increase at $\epsilon = 0.018$, Fig. 7 (m)-(p), the response oscillator system responds not only to the single peaks of the driver oscillator system, causing a change from the Rössler attractor to the Homoclinic attractor in the response oscillator system but also to the phase oscillation when the system remains in the similar attractors. It is noteworthy that phase synchronization is always accompanied by delay synchronization, where the shift time $\tau > 0$ of the similarity function is positive and the minimum S_{min} of this function also decreases $S \approx 1$, see Fig. 7 (p), which means that the response and drive oscillator systems reach phase synchronization, with the phase difference $\theta_{i,j}$ reaching $\theta_{i,j} \approx 0$, see Fig. 7 (n), and while the time series Fig. 7 (n) show that the delayed phase synchronization of the driver and response oscillator system has been achieved. For stronger coupling parameter $\epsilon_2 > 0.02$ the response oscillator system becomes unstable and there is no numerical solution the of the equation system (1).

Similar work on synchronization of a multistable system was done by Pisarchik *et al.* (2008). In this work, the authors show a detailed study of synchronizing two unidirectionally coupled identical systems with coexisting chaotic attractors and analyze the system dynamics observed on the route from asynchronous behavior to complete synchronization when the coupling strength is increased. In contrast to our work, they have studied two similar coexisting chaotic Rössler attractors. However, in the present work, we study the phase synchronization of two different chaotic attractors: the Homoclinic chaotic attractor and Rössler chaotic attractor. Because the system of equations (1) becomes unstable, complete synchronization was not found for the stronger coupling parameter $\epsilon > 0.02$. In Fig. 8 (a), the average synchronization error, see system equation (9) as a function of the coupling strength ϵ is shown. This figure shows that the synchronization error e increases when the control parameter ϵ is increased, i.e., complete synchronization between driver and response oscillator systems was not found. On the other hand, Fig. 8 (b) shows the average phase synchronization $< \theta_{i,j} >$ as a function of the coupling strength ϵ, where we can see that $< \theta_{i,j} >$ approaches zero when the control parameter ϵ is increased, indicating that phase or delay phase synchronization has been achieved.

Similarly, the bifurcation diagram of the local maximum of the state variables x_1 driver and x_2 response oscillator are shown in Figs. 9(a) and (b), respectively, as a function of the coupling strength ϵ. In this figure, we can see when the response oscillator system (Fig. 9 (b)) jumps from the Rössler chaotic attractor **R** to a new Homoclinic chaotic attractor $\mathbf{H}_2$, which is different from the Homoclinic chaotic attractor $\mathbf{H}_1$ of the driver oscillator system, i.e., there is a critical value of coupling strength $\epsilon_c = \epsilon = 0.005$ at which the response oscillator system changes its local maximum from $x_2^{max} \approx 3.6$ (Rössler attractor) to $x_2^{max} \approx 4.3$ (Homoclinic attractor $\mathbf{H}_2$).

Case (b) driver system in Rössler chaotic attractor and response system in Homoclinic chaotic attractor

Similar to the synchronization analysis performed in the Figs. 7 -9, in the Figs. 10- 12, a synchronization analysis is also performed, but in this case, we have the initial condition for the driver oscillator system equations.

The initial condition for the system Eqs.1 or Eqs.2 representing a

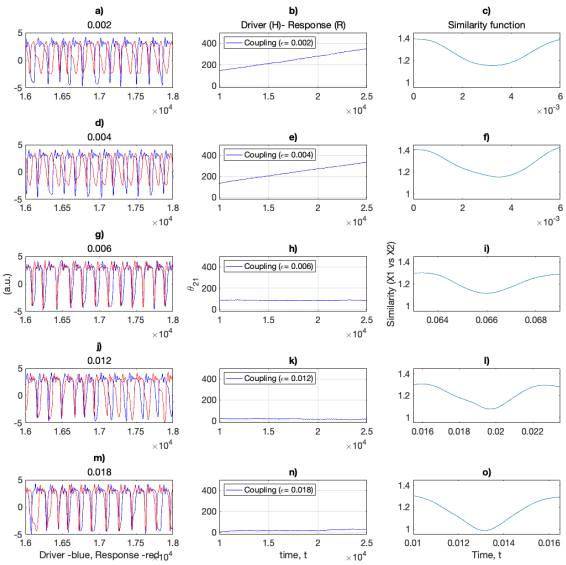

Figure 7 The time series of the coupled variables x_1, x_2 (left) and the phase difference $\theta_{i,j}$ (center) and Similarity Function (right).

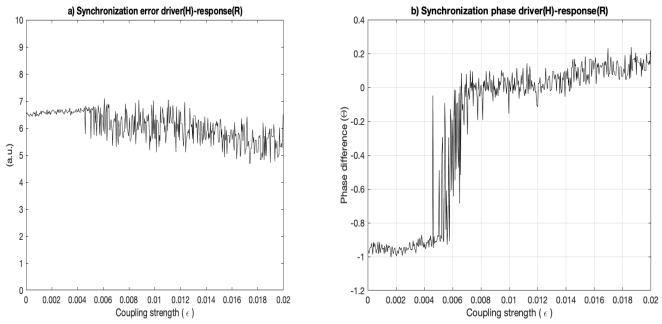

Figure 8 Show the average synchronization error equation system $< e_{i,j} >$ equation (9) as function of the coupling strength ϵ, the average phase synchronization $< \theta_{i,j} >$ as function of the coupling strength ϵ.

Homoclinic chaotic attractor **H** is reached using I.C.: $x_{10} = 2.38019$, $y_{10} = -5.31956$ and $z_{10} = 2.32858$, see Fig. 6a and showing a Rössler chaotic attractor **R** is reached using I.C.: $x_{20} = 3.034636$, $y_{20} = -4.64063$ and $z_{20} = 0.00920$ see Fig. 6b.

Eqs. 1 representing the Rössler chaotic oscillator **R** (I.C. $x_{20} = 3.034636$, $y_{20} = -4.64063$ and $z_{20} = 0.00920$) and while the initial condition of the response system represents a Homoclinic chaotic oscillator $\mathbf{H}_1$ (I. C. $x_{10} = 2.38019$, $y_{10} = -5.31956$ and $z_{10} = 2.32858$). The time series of the coupled variables x_1 and x_2, the phase difference $\theta_{i,j}$, and the similarity function $S_{i,j}(\tau)$ for different values of the coupling strength (ϵ) are shown in Fig. 10. In this figure, we can see that the phase synchronization was not achieved. Similarly, the average error synchronization $< e >$ and the average phase synchronization $< \theta_{i,j} >$ as a function of the coupling strength ϵ are shown in the Fig. 11 (a),(b) respectively, where no complete and no phase synchronization was found.

Also, the bifurcation diagrams of the local maximum of the state variables x_1 drive and x_2 response are shown in Fig. 12 (a)

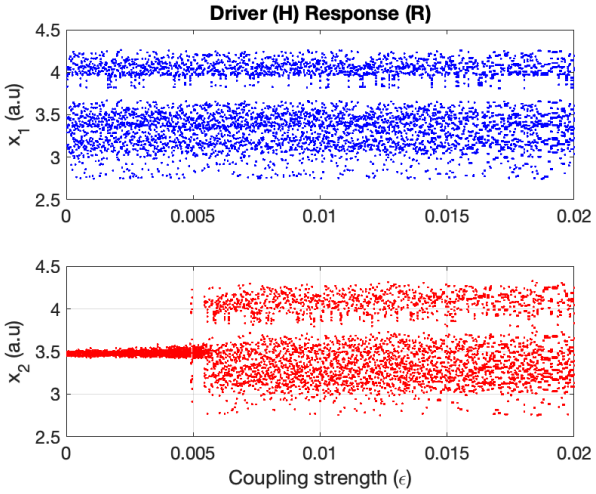

Figure 9 The bifurcation diagram of the local max of the state variables x_1 and x_2 as a function of the coupling strength ϵ.

and (b), respectively, as a function of the coupling strength ϵ. It can be observed that there is no critical value for the coupling strength ϵ_c at which the response oscillator system changes its local maximum from the x_2^{max} form of the Homoclinic attractor to the x_2^{max} Rössler attractor. It is worth noting that for larger values of the coupling strength ϵ the response oscillator system has no solution or it becomes an unstable system.

Thus, this result indicates an opposition to the synchronization of the response oscillator system when it operates as a Homoclinic chaotic attractor and the driver oscillator system operates as a Rössler chaotic attractor. Remarkably, to our knowledge, this is the first study of the opposition to the synchronization of bistable chaotic oscillator systems. In particular, the Homoclinic chaotic attractor of the response oscillator system resists entrainment or synchronization with the Rössler signal of the driver oscillator system. In contrast, in the cases where the response oscillator system is fixed in the Rössler chaotic attractor and the driver oscillator system is fixed in the Homoclinic chaotic attractor, there is a threshold coupling strength ϵ at which the Rössler chaotic attractor jump a new Homoclinic chaotic attractor and, depending on the coupling strength, the driver-response oscillator systems achieves delayed phase synchronization.

SYNCHRONIZATION OF THREE IDENTICAL RÖSSLER OSCILLATOR SYSTEMS COUPLED IN MOTIF CONFIGURATION.

In this work, we also study opposition to synchronization of multistable systems for another type of coupling, such as motif configuration of three identical bistable Rössler oscillator systems unidirectionally coupled. For example, two driver oscillator systems coupled to one response oscillator system, see equation systems Eqs.3, Eqs.4 and Eqs.5 where the two driver oscillator systems operate as a Rössler chaotic attractor and the response oscillator system operates in Homoclinic chaotic attractors, see the Fig.13.a) and Fig.14.a) for the average error synchronization $< e_{i,j} >$, and the average phase synchronization $< \theta_{i,j} >$ respectively, and also the Fig.15.a) the bifurcation diagrams of the local maximum of the state variables x_1 driver and x_2 response oscillator, as a function of the coupling strength ϵ. In these figures, it is clear that com-

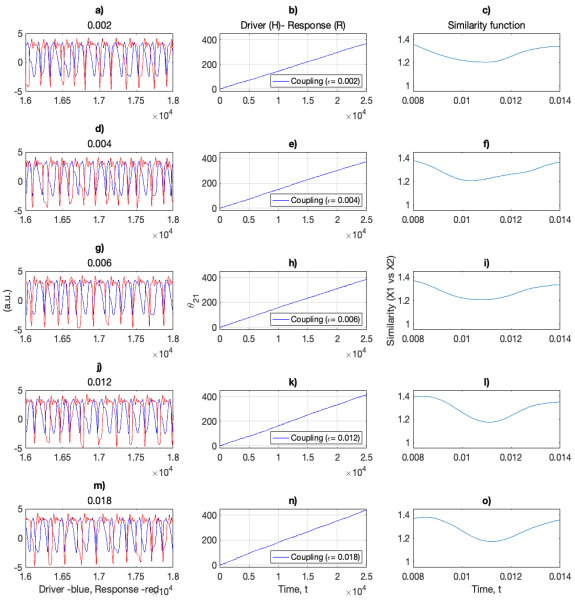

Figure 10 The time series of the coupled variables x_1 (left), x_2 and the phase difference $\theta_{i,j}$ (center) and Similarity Function (right).

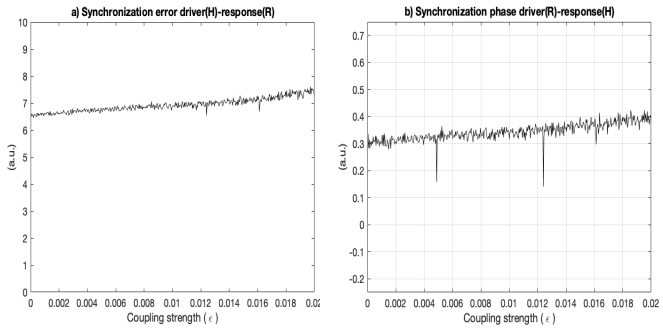

Figure 11 Show the average synchronization error equation system $< e_{i,j} >$ equation (9) as function of the coupling strength ϵ, the average phase synchronization $< \theta_{i,j} >$ as function of the coupling strength ϵ.

plete and phase synchronization between the driver and response oscillator systems has not been achieved.

In contrast, when the two driver oscillator systems operate in the Homoclinic chaotic attractor and the response oscillator system operates in the Rössler chaotic attractor, delayed phase synchronization between the driver and response oscillator systems is achieved since a value threshold of coupling strength ϵ. To observe these results, see Fig.13.b), Fig.14.b) and Fig.15.b) for the bifurcation diagrams, the average error synchronization $< e_{i,j} >$, and the average phase synchronization $< \theta_{i,j} >$ respectively.

In addition, this study also considered the opposition to synchronization of bistable chaotic oscillator systems in a configuration ring with unidirectional coupling schemes, where all oscillators act simultaneously as drivers and as response oscillator systems, see equation systems Eqs.6, Eqs.7 and Eqs.8. In this

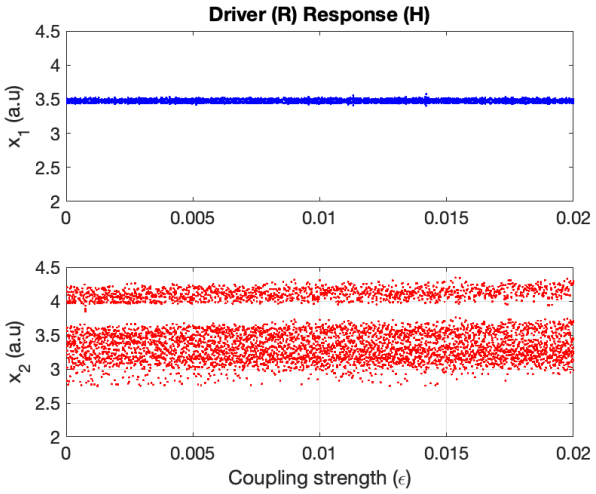

Figure 12 The bifurcation diagram of the local max of the state variables x_1 and x_2 as a function of the coupling strength ϵ.

configuration, it is sufficient for only one oscillator operating in Homoclinic chaotic attractors to trigger the entrainment of other two oscillators operating in Rössler chaotic attractors jump to new Homoclinic chaotic attractor since a value threshold of coupling strength ϵ.

The following figures show the dependence of the average error synchronization $< e_{i,j} >$ see Fig. 16 a), b), the average phase synchronization $< \theta_{i,j} >$ see Fig. 17 a),b), and the bifurcation diagrams of the local maximum of the state variables x_1 driver and x_2 response oscillator systems in Fig. 18 a), b), for the coupling strength ϵ. This means that all oscillators achieve synchronization in phase synchronization. This is an unexpected result since one might expect that these two oscillator systems operating in the Rössler chaotic attractor should cause the other oscillator operating in the Homoclinic chaotic attractor to jump to the Rössler chaotic attractor and that all oscillators should be able to synchronize in-phase synchronization.

The above result shows that the Homoclinic chaotic attractor opposes synchronization with Rössler chaotic attractor. In contrast, the homoclinic chaotic attractor is the one that stimulates the other two oscillators operating in the Rössler chaotic attractor to jump to the new Homoclinic chaotic attractor and then all these oscillators achieve phase synchronization.

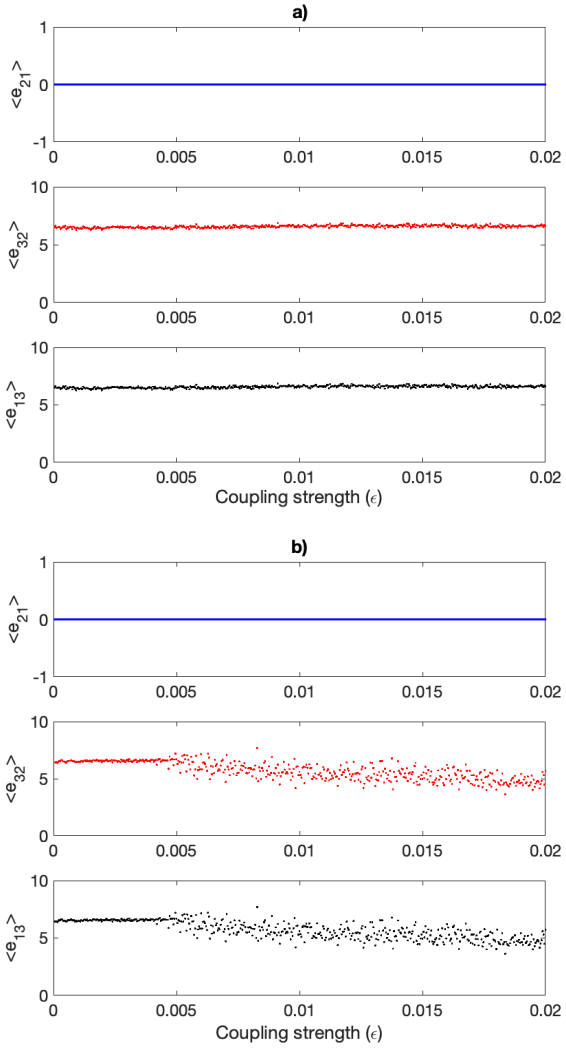

Figure 13 Synchronization error as function of the coupling strength (ϵ), a) Two drivers Rössler type, one response Homoclinic type, b) Two drivers Homoclinic type, one response Rössler type.

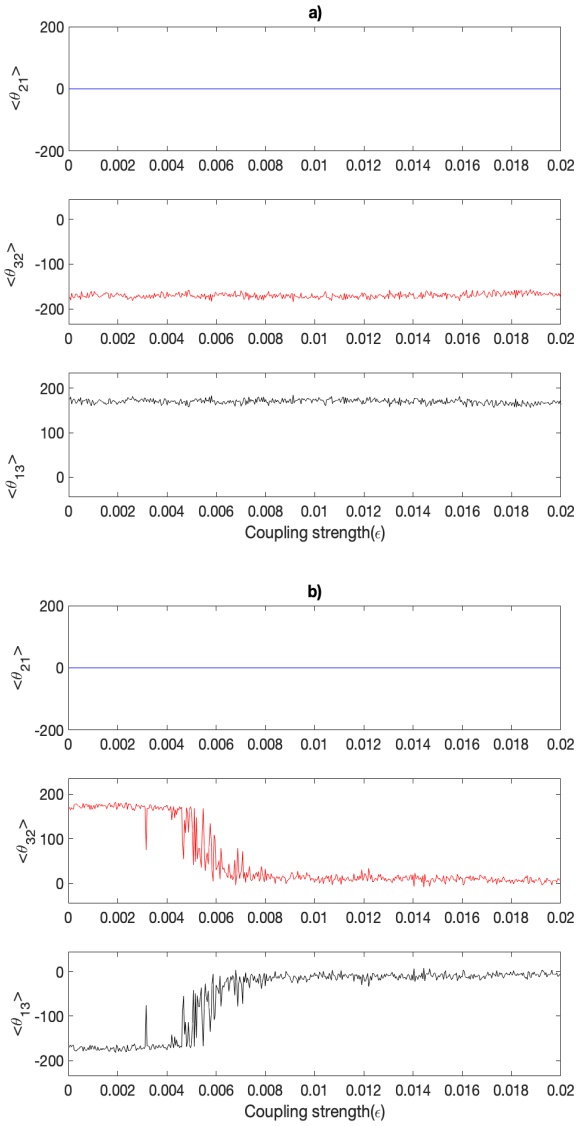

Figure 14 Phase synchronization as function of the coupling strength (ϵ), a) Two drivers Rössler type, one response Homoclinic type, b) Two drivers Homoclinic type, one response Rössler type.

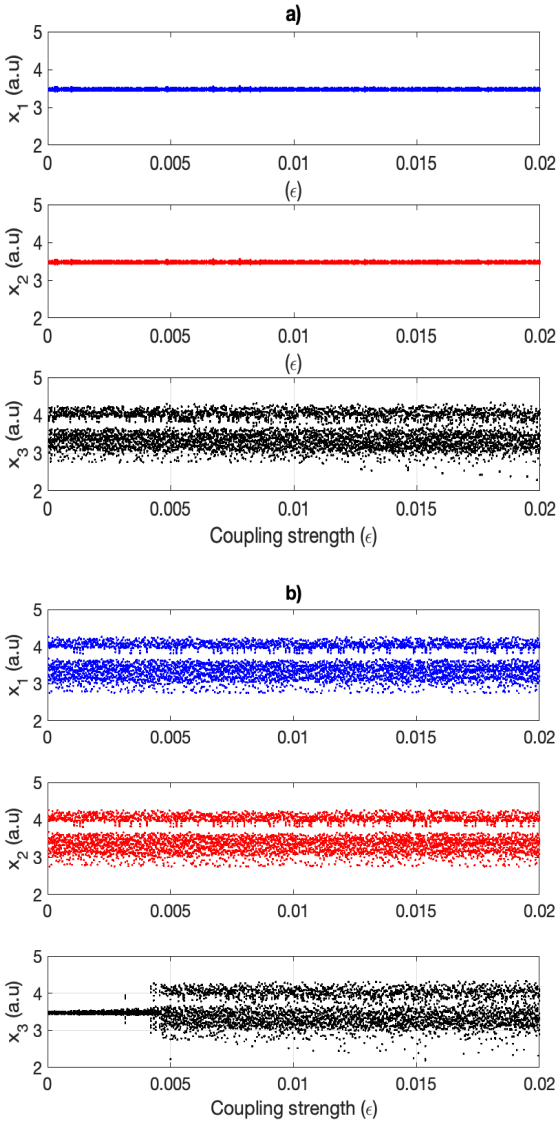

Figure 15 The bifurcation diagram of the local max of the state variables x_1, x_2 and x_3 as function of the coupling strengthϵ, a) Two drivers Rössler type, one response Homoclinic type, b) Two drivers Homoclinic type, one response Rössler type.

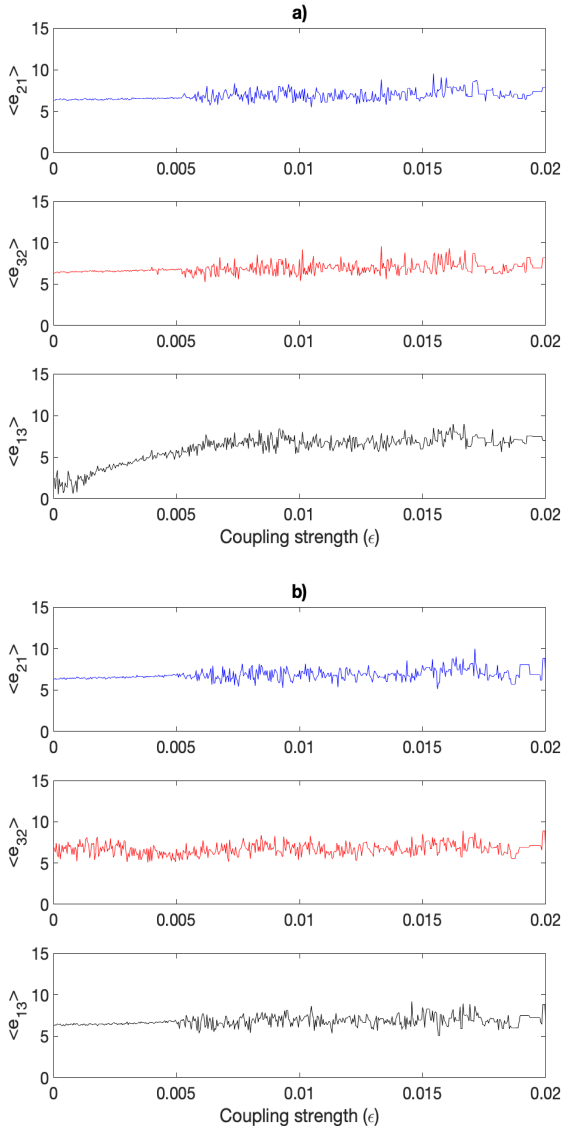

Figure 16 Synchronization error as function of the coupling strength (ϵ), a) Ring with two Rössler type, one Homoclinic type, b) Ring with two Homoclinic type, one Rössler type.

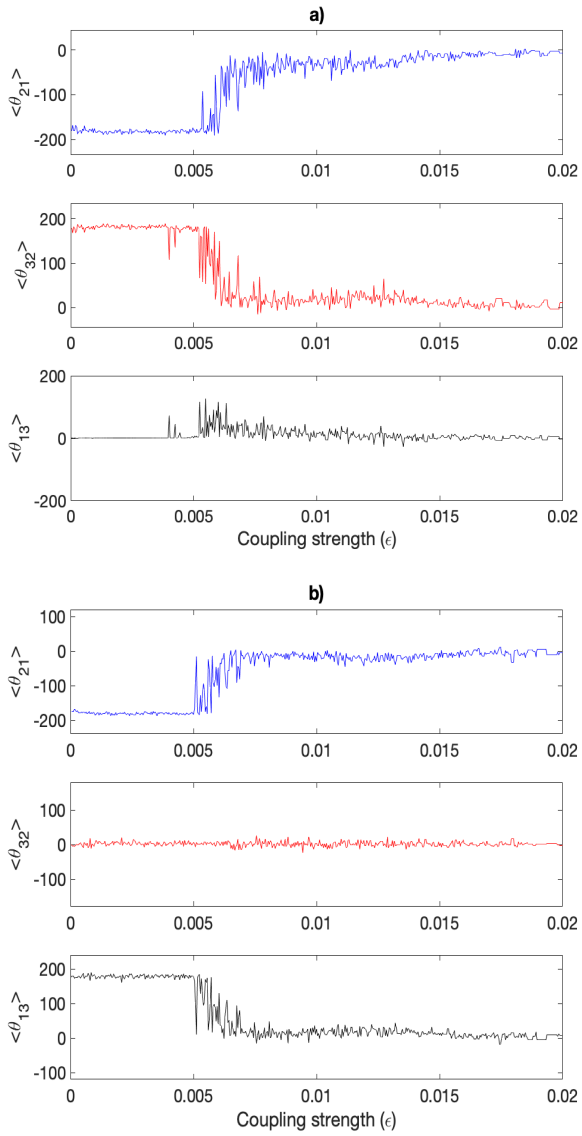

Figure 17 Phase synchronization as function of the coupling strength (ϵ), a) Ring with two Rössler type, one Homoclinic type, b)Ring with two Homoclinic type, one Rössler type.

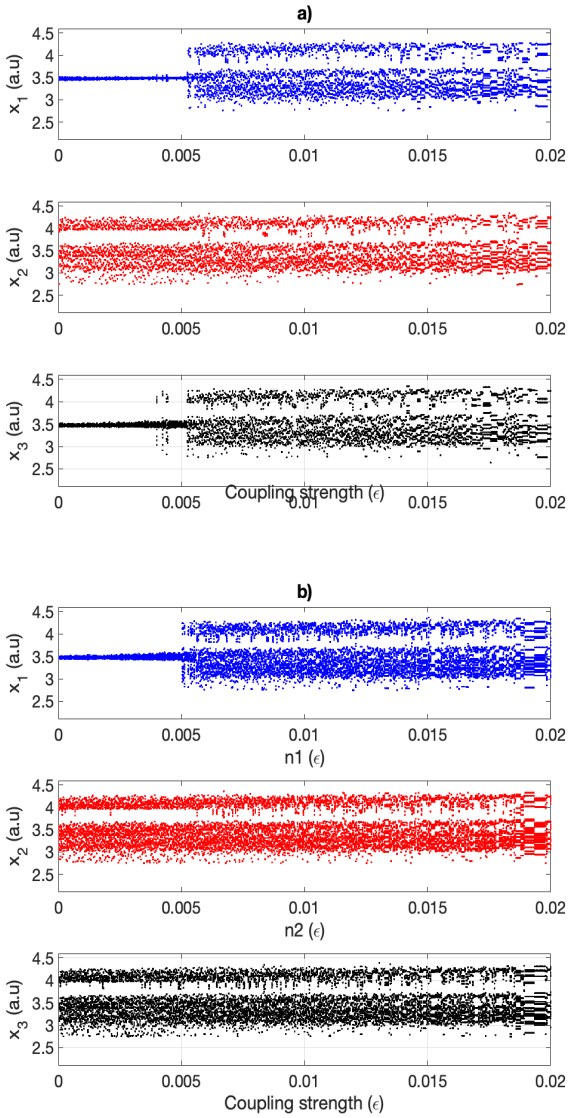

Figure 18 The bifurcation diagram of the local max of the state variables x_1, x_2 and x_3 as function of the coupling strengthϵ, a) Ring with two Rössler type, one Homoclinic type, b) Ring with two Homoclinic type, one Rössler type.

CONCLUSION

We have performed numerical investigations with Rössler oscillator system the opposition to synchronization of a bistable chaotic dynamical system coupled in different configurations: (a) two identical bistable chaotic oscillators coupled in a driver and a response system; (b) three identical bistable chaotic oscillators coupled in motif configuration; two drivers and one response oscillator, and (c) three identical coupled oscillators in a ring configuration where all oscillators act together as driver and response system. We have chosen the initial conditions of the driver or response oscillator system to be either a Homoclinic chaotic attractor or a Rössler chaotic attractor. In the first (a) case, when the driver oscillator system operates in the regime of the Homoclinic chaotic attractor and the response oscillator system in the regime of the Rössler chaotic attractor, there is a critical value of the coupling strength $\epsilon_c = \epsilon = 0.005$ at which the response oscillator system jumps from the Rössler chaotic attractor $\mathbf{R}$ to a new Homoclinic chaotic attractor $\mathbf{H}_2$ that is different from the Homoclinic chaotic attractor $\mathbf{H}_1$ of the driver oscillator system, i.e., the response oscillator system is sensitive to the driver signal.

Further increasing the coupling parameter $\epsilon > 0.005$, the phase synchronization is most evident where the response oscillator system remains into a homoclinic chaotic attractor, which is similar to the attractor of the driver oscillator system. An unexpected result was found when the driver oscillator system operates in the Rössler chaotic attractor regime and the response oscillator system operates into the Homoclinic chaotic attractor regime, as one might expect the driver oscillator system to cause the response oscillator system to jump to the Rössler chaotic attractor and the driver response oscillator system to be able to synchronize in phase, but this was not found. On the contrary, the result shows that the Homoclinic chaotic attractor opposes synchronization with Rössler chaotic attractor. The above results are because the basin attraction of the Homoclinic chaotic attractor is greater than the basin attraction of the Rössler chaotic attractor. When the response system operating in the homoclinic regime receives the signal of the Rössler chaotic attractor from the driver system, the response oscillator system does not change the attractor but maintains its original regime of the Homoclinic chaotic attractor, so that synchronization between the Homoclinic and Rössler chaotic attractors is not possible.

In contrast, the basin of attraction of the Rössler chaotic attractor is smaller than that of the Homoclinic chaotic attractor. When the response system operating in the Rössler chaotic attractor receives the homoclinic signal from the driver oscillator system, the response oscillator system is sensitive to the signal from the driver oscillator system, which acts like an external signal and causes the response oscillator system to jump from the Rössler chaotic attractor to the Homoclinic chaotic attractor, achieving the phase synchronization regime between the driver and response oscillator systems. A similar result was found regarding the opposition of the Homoclinic chaotic attractor to synchronization with the Rössler attractors when the network of three coupled bistable chaotic dynamical systems is considered: (b) three identical bistable chaotic oscillators coupled in motif configuration; two drivers and one response oscillator, and (b) three identical coupled oscillators in a ring configuration where all oscillators act together as driver and response oscillator system.

Acknowledgments

This work was supported by the University of Guadalajara, CU-Lagos, DCET. R.J.R. acknowledges to the National Council of Humanities, Science, and Technology (CONAHCYT), Project Number 320597.

Availability of data and material

Not applicable.

Conflicts of interest

The authors declare that there is no conflict of interest regarding the publication of this paper.

Ethical standard

The authors have no relevant financial or non-financial interests to disclose.

LITERATURE CITED

Ahmed, H., R. Ushirobira, D. Efimov, and W. Perruquetti, 2016 Robust synchronization for multistable systems. IEEE Transactions on Automatic Control **61**: 1625–1630.

Boccaletti, S., 2008 The synchronized dynamics of complex systems. Monograph series on nonlinear science and complexity **6**: 1–239.

Boccaletti, S., L. M. Pecora, and A. Pelaez, 2001 Unifying framework for synchronization of coupled dynamical systems. Physical Review E **63**: 066219.

Boccaletti, S., A. N. Pisarchik, C. I. Del Genio, and A. Amann, 2018 *Synchronization: from coupled systems to complex networks*. Cambridge University Press.

Brun, E., B. Derighetti, D. Meier, R. Holzner, and M. Ravani, 1985 Observation of order and chaos in a nuclear spin–flip laser. JOSA B **2**: 156–167.

Buldú, J. M., T. Heil, I. Fischer, M. C. Torrent, and J. García-Ojalvo, 2006 Episodic synchronization via dynamic injection. Physical review letters **96**: 024102.

Carroll, T. L. and L. M. Pecora, 1995 *Nonlinear dynamics in circuits*. World Scientific.

Chakraborty, P. and S. Poria, 2019 Extreme multistable synchronisation in coupled dynamical systems. Pramana **93**: 1–13.

Dudkowski, D., K. Czołczyński, and T. Kapitaniak, 2021 Multistable synchronous states of two pendulum clocks suspended on a swinging support. Mechanical Systems and Signal Processing **154**: 107549.

Farkas, I., D. Helbing, and T. Vicsek, 2002 Mexican waves in an excitable medium. Nature **419**: 131–132.

Foss, J., A. Longtin, B. Mensour, and J. Milton, 1996 Multistability and delayed recurrent loops. Physical Review Letters **76**: 708.

García-Guerrero, E., E. Inzunza-González, O. López-Bonilla, J. Cárdenas-Valdez, and E. Tlelo-Cuautle, 2020 Randomness improvement of chaotic maps for image encryption in a wireless communication scheme using pic-microcontroller via zigbee channels. Chaos, Solitons and Fractals **133**: 109646.

Gauthier, D. J. and J. C. Bienfang, 1996 Intermittent loss of synchronization in coupled chaotic oscillators: Toward a new criterion for high-quality synchronization. Physical Review Letters **77**: 1751.

Khan, M. A., G. Mahapatra, J. K. Sarkar, and S. D. Jabeen, 2021 Design of multistability of chaotic systems via self and cross coupling. The European Physical Journal Plus **136**: 1–12.

Khan, M. A., M. Nag, and S. Poria, 2017 Design of multistable systems via partial synchronization. Pramana **89**: 1–8.

Liu, W., J. Xiao, X. Qian, and J. Yang, 2006 Antiphase synchronization in coupled chaotic oscillators. Physical Review E **73**: 057203.

Maurer, J. and A. Libchaber, 1980 Effect of the prandtl number on the onset of turbulence in liquid 4he. Journal de Physique lettres **41**: 515–518.

Méndez-Ramírez, R., A. Arellano-Delgado, and M. Á. Murillo-Escobar, 2023 Network synchronization of macm circuits and its application to secure communications. Entropy **25**: 688.

Moskalenko, O. I., A. A. Koronovskii, A. O. Selskii, and E. V. Evstifeev, 2021 On multistability near the boundary of generalized synchronization in unidirectionally coupled chaotic systems. Chaos: An Interdisciplinary Journal of Nonlinear Science **31**: 083106.

Pecora, L. M. and T. L. Carroll, 1990 Synchronization in chaotic systems. Physical review letters **64**: 821.

Pikovsky, A., M. Rosenblum, J. Kurths, *et al.*, 2001 A universal concept in nonlinear sciences. Self **2**: 3.

Pisarchik, A., R. Jaimes-Reátegui, J. Villalobos-Salazar, J. Garcia-Lopez, and S. Boccaletti, 2006 Synchronization of chaotic systems with coexisting attractors. Physical review letters **96**: 244102.

Pisarchik, A. N. and R. Jaimes-Reategui, 2005 Intermittent lag synchronization in a nonautonomous system of coupled oscillators. Physics Letters A **338**: 141–149.

Pisarchik, A. N., R. Jaimes-Reátegui, and J. García-López, 2008 Synchronization of multistable systems. International Journal of Bifurcation and Chaos **18**: 1801–1819.

Pisarchik, A. N., A. V. Kir'yanov, Y. O. Barmenkov, and R. Jaimes-Reátegui, 2005 Dynamics of an erbium-doped fiber laser with pump modulation: theory and experiment. JOSA B **22**: 2107–2114.

Pm, G. and T. Kapitaniak, 2017 Synchronization in coupled multistable systems with hidden attractors. Mathematical Problems in Engineering **2017**.

Pol, B. and J. v. d. Mark, 1927 Frequency demultiplication. Nature **120**: 363–364.

Rodríguez-Orozco, E., E. E. García-Guerrero, E. Inzunza-Gonzalez, O. R. López-Bonilla, A. Flores-Vergara, *et al.*, 2018 Fpga-based chaotic cryptosystem by using voice recognition as access key. Electronics **7**.

Rosenblum, M. and J. Kurths, 2003 *Synchronization: a universal concept in nonlinear science*. Cambridge University Press.

Rosenblum, M. G., A. S. Pikovsky, and J. Kurths, 1996 Phase synchronization of chaotic oscillators. Physical review letters **76**: 1804.

Rosenblum, M. G., A. S. Pikovsky, and J. Kurths, 1997 From phase to lag synchronization in coupled chaotic oscillators. Physical Review Letters **78**: 4193.

Ruiz-Silva, A., H. Gilardi-Velázquez, and E. Campos, 2021 Emergence of synchronous behavior in a network with chaotic multistable systems. Chaos, Solitons & Fractals **151**: 111263.

Rulkov, N. F., M. M. Sushchik, L. S. Tsimring, and H. D. Abarbanel, 1995 Generalized synchronization of chaos in directionally coupled chaotic systems. Physical Review E **51**: 980.

Sarosh, P., S. A. Parah, and G. M. Bhat, 2022 An efficient image encryption scheme for healthcare applications. Multimedia Tools and Applications **81**: 7253–7270.

Sharma, N. and E. Ott, 2000 Exploiting synchronization to combat channel distortions in communication with chaotic systems. International Journal of Bifurcation and Chaos **10**: 777–785.

Stewart, H. B., R. Ghaffari, C. Franciosi, and H. Swinney, 1986 *Nonlinear dynamics and chaos: geometrical methods for engineers and scientists*. Wiley New York.

Trujillo-Toledo, D., O. López-Bonilla, E. García-Guerrero, J. Esqueda-Elizondo, J. Cárdenas-Valdez, *et al.*, 2023 Real-time medical image encryption for h-iot applications using improved sequences from chaotic maps. Integration **90**: 131–145.

Vaidyanathan, S., K. Benkouider, and A. Sambas, 2022 A new multistable jerk chaotic system, its bifurcation analysis, backstepping control-based synchronization design and circuit simulation. Archives of Control Sciences **32**: 123.

How to cite this article: García-López, J. H., Jaimes-Reátegui, R., Huerta-Cuellar, G. and López-Mancilla D. Opposition to Synchronization of Bistable State in Motif Configuration of Rössler Chaotic Oscillator Systems. *Chaos Theory and Applications*, 6(2), 131-143, 2023.